



ELSEVIER

Physica C 280 (1997) 1–8

PHYSICA C

Regions of enhanced pinning in the mixed state of the superconductor $\text{Yb}_3\text{Rh}_4\text{Sn}_{13}$

C.V. Tomy, G. Balakrishnan *, D.McK. Paul

Department of Physics, University of Warwick, Coventry CV4 7AL, UK

Received 7 January 1997; revised 27 February 1997; accepted 16 April 1997

Abstract

We present results of magnetisation, electrical resistivity and critical current measurements in applied magnetic fields on single crystals of the superconductor, $\text{Yb}_3\text{Rh}_4\text{Sn}_{13}$. An irreversible peak is observed in the magnetisation, at high fields below H_{c2} . Evidence for a region of enhanced pinning is obtained from resistance measurements in magnetic fields. The temperature and field region where these anomalies are observed have been mapped. The anomalous features seen in the magnetisation and resistance measurements extend to $T \sim 0.9T_c$. The results presented here for $\text{Yb}_3\text{Rh}_4\text{Sn}_{13}$ resemble those obtained for CeRu_2 , which is considered a candidate for the observation of the Fulde-Ferrel-Larkin-Ovchinnikov state. © 1997 Elsevier Science B.V.

Keywords: Superconductivity; Peak effect; Stannides; Pinning

1. Introduction

$\text{Yb}_3\text{Rh}_4\text{Sn}_{13}$ belongs to the family of ternary stannides that exhibit superconductivity, magnetism and the coexistence of superconductivity with magnetism [1]. One of the compounds in this series, $\text{Er}_3\text{Rh}_4\text{Sn}_{13}$ shows re-entrant superconductivity for certain compositions. $\text{Yb}_3\text{Rh}_4\text{Sn}_{13}$ forms as phase I, (primitive cubic) or in a distorted phase I (phase IV) [2]. There are two different sites for the Sn atom in this crystal structure and the formula is generally written as $\text{Sn}(1)\text{Yb}_3\text{Rh}_4\text{Sn}(2)_{12}$ [2]. It is also known to form in phase II/III (pseudo-tetragonal/face centred cubic) due to the atomic disorder between the Sn(1) and Yb positions [3]. $\text{Yb}_3\text{Rh}_4\text{Sn}_{13}$ shows su-

perconductivity with T_c values ranging from 7–8 K for crystals adopting the cubic structure (phase I), while samples with phase II/III structures are not superconducting.

Recently, Sato et al. [4] have reported the observation of a 'peak effect' in $\text{Yb}_3\text{Rh}_4\text{Sn}_{13}$. They observed an irreversible peak in the magnetisation just below H_{c2} , which is a characteristic of the 'peak effect' in superconductors. In a number of experiments, such anomalies in the magnetisation have been observed in the mixed state of both conventional and high temperature superconductors and are thought to be related to an increase in the pinning of the flux-line lattice above a certain applied magnetic field. These anomalies are either understood as being due to the change in the critical current density, giving rise to a conventional 'peak effect' [5–7], or as a signature of the Fulde-Ferrel-Larkin-Ovchinnikov

* Corresponding author. Tel.: +44 1203 523356; fax: +44 1203 692016; e-mail: phryj@csv.warwick.ac.uk

kov (FFLO) state proposed by Fulde and Ferrel [8] and Larkin and Ovchinnikov [9] independently. The former is widely observed in a number of superconductors and the origin is reasonably well understood in most cases, while the latter has not been observed in conventional superconductors, but certain candidates amongst heavy fermion superconductors have been suggested [10].

The phase diagram obtained by Sato et al. [4] for $\text{Yb}_3\text{Rh}_4\text{Sn}_{13}$ from their magnetisation measurements closely resembles that of CeRu_2 , which in addition to showing the same irreversible peak in magnetisation [11], also presents features in magnetostriction, AC susceptibility and elastic constants measurements in an applied magnetic field [12]. These observations in CeRu_2 have been taken as an indication of the existence of the FFLO state. The FFLO state has been searched for in other heavy fermion superconductors such as UPd_2Al_3 and CeCo_2 [10,12]. All these compounds satisfy the conditions put forward originally to observe the FFLO state, i.e. they are 'clean superconductors', where $l \gg \xi$, (l is the mean free path and ξ is the coherence length) and are strongly Pauli limited superconductors. From the results of magnetisation and magneto-transport measurements on these heavy fermion superconductors, it has often been difficult to establish whether the 'peak' in the magnetisation curves is due to the first order transition from the conventional superconducting state to the FFLO state, or whether it is the 'conventional peak effect' that is brought about by a plastic deformation of the flux-line lattice around pinning sites.

Given the similarities in the magnetisation curves of $\text{Yb}_3\text{Rh}_4\text{Sn}_{13}$ and CeRu_2 , it is of interest to investigate, in greater detail, the magneto-transport behaviour of $\text{Yb}_3\text{Rh}_4\text{Sn}_{13}$ in the mixed state in an attempt to establish the origin of the peak effect observed in the magnetisation measurements. We present results of magnetisation, electrical resistance and critical current measurements in applied magnetic fields on single crystals of $\text{Yb}_3\text{Rh}_4\text{Sn}_{13}$. The results obtained allow us to construct a phase diagram showing the transition from a weakly pinned regime to a strongly pinned regime in the H - T phase diagram. We present evidence for a region of enhanced pinning at high fields, from resistance measurements in an applied magnetic field.

2. Experimental details

Single crystals of $\text{Yb}_3\text{Rh}_4\text{Sn}_{13}$ were prepared by the tin flux method [13]. Magnetisation measurements were performed using a SQUID magnetometer with a scan length of 4 cm and a vibrating sample magnetometer (VSM). For the resistance measurements, a sample with dimensions of $0.22 \times 0.42 \times 2.38 \text{ mm}^3$, was cut out from one of the crystals which was used for the magnetisation measurements. A four probe DC method was employed for measuring the electrical resistance. The measuring currents were between 1–100 mA, where 1 mA corresponds to a current density of $J = 1 \text{ A cm}^{-2}$. No anomalous features were observed in a longitudinal geometry with the current parallel to the applied magnetic field and therefore for all the measurements described in this work the current was applied perpendicular to the direction of the applied magnetic field to permit such measurements to be sensitive to the Lorentz force on the pinned flux. For a given temperature and measuring current, the magnetic field dependence of the electrical resistance $R(H)$ was measured by increasing or decreasing the field to fixed values. The temperature variation of the resistance $R(T)$ was measured over fixed intervals of temperature at a given magnetic field and current. The measurements were carried out for decreasing as well as increasing temperatures after cooling the sample either in zero field or an applied field. The critical current values (I_c) were obtained from the I - V characteristics at fixed temperature and field.

3. Results and discussion

The crystals obtained from the growth were found to be superconducting with T_c values ranging from 7–8 K. Magnetisation measurements were performed on four different crystals and identical results were obtained for all the crystals. The M vs. H curves for one of the crystals (with a T_c of 7.2 K) are shown in Fig. 1. The M vs. H scans were measured using both the SQUID and the VSM and found to be identical for both types of measurements, ruling out the possibility of any artefacts arising from the inhomogeneity of the field as a result of the movement of the sample in the SQUID measurement [11]. The

magnetisation curves show a marked dip at a particular field value, H^* , before the upper critical field H_{c2} is reached. The H_{c2} and H^* values obtained from this measurement agree well with that reported by Sato et al. [4]. This feature in the magnetisation is also reported for UPd_2Al_3 , CeRu_2 , CeCo_2 [12] as well as in a number of conventional superconductors [6,14]. In the conventional superconductors, this is attributed to the peak effect, which is a manifestation of an increase in the critical current to a maximum before falling to zero at H_{c2} , due to the ability of the flux-line lattice to more easily distort around pinning sites in this field range [5], whereas in the former superconductors, it has been interpreted as evidence for a possible FFLO state [12]. In both scenarios, however, the source of the peak is from a rearrangement in the pinned configuration of flux.

In order to investigate whether this peak in magnetisation is related to an increase in the critical current, measurements of the resistance (at fixed applied current) as well as critical current as a function of temperature and magnetic field were carried out. Fig. 2 shows the resistance variation with temperature on a single crystal of $\text{Yb}_3\text{Rh}_4\text{Sn}_{13}$, for various applied magnetic fields and a fixed measuring current of $I = 40$ mA. In zero applied field, the superconducting transition is illustrated by the resistance, R , dropping to zero and remaining at zero to the lowest temperature measured. As the applied

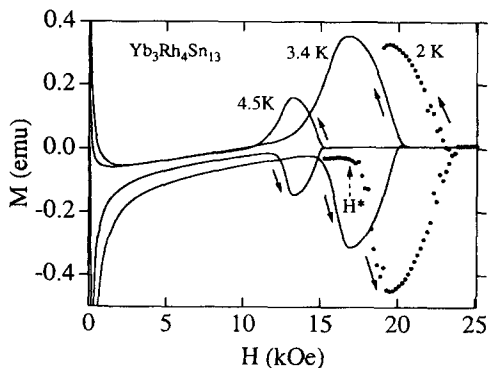


Fig. 1. Magnetisation as a function of applied magnetic field for a single crystal of $\text{Yb}_3\text{Rh}_4\text{Sn}_{13}$. The 2 K data is from the SQUID measurement whereas the 3.4 K and 4.5 K data are from the VSM measurements. The arrows indicate the increasing and decreasing field directions. H^* denotes the field at which the onset of the peak in M vs. H occurs.

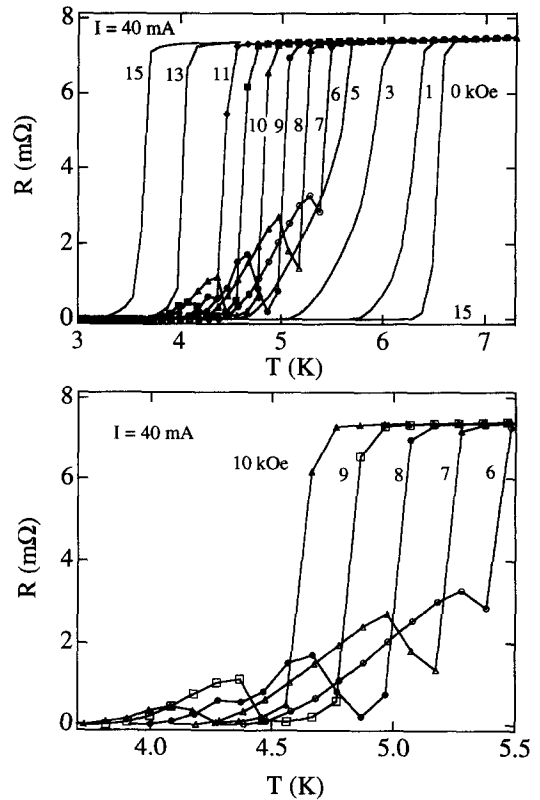


Fig. 2. (a) Resistance as a function of temperature for different applied fields (0–15 kOe). The measuring current is 40 mA. (b) Expanded version to highlight the peaks occurring between 6–10 kOe.

magnetic field is increased, a sudden increase in resistance is seen for a certain range of magnetic fields, after the onset of the superconducting transition, just before the resistance tails off to zero. This sudden increase in resistance is observed for fields between 6–10 kOe for this current value. The curves are identical for both increasing and decreasing temperatures, showing no hysteresis. For magnetic field values of 9 and 10 kOe, the resistance drops to zero before increasing to a finite value, while for other fields, the resistance just shows a dip before increasing and then gradually falling to zero. As the measuring current is varied, the temperature and the field at which the rise in $R(T)$ occurs changes and this observation is discussed in the following sections. These measurements will only reflect an increase in the pinning strength and hence the ability of the flux

distribution to remain static against the Lorentz force, if the flux is already flowing before entering the new region of increased pinning. If the pinning in the more reversible region (lower field) is sufficiently strong to prevent the flux moving under the Lorentz force then there will be no anomaly detected on entering the stronger pinning region at higher field in such resistance measurements. The magnitude of the change in the degree of dissipation due to flux movement will depend on the contrast in pinning between the two regions.

Fig. 3 shows the resistance (R) vs. magnetic field (H) curves at a fixed temperature for different values of the measuring current through the sample. At 2.9 K, the increase in resistance is seen for currents between 60 and 90 mA appearing at fields between 11 and 6 kOe. With the current through the sample fixed at 50 mA (a value at which no dip or rise in R is observed at 2.9 K), the temperature was increased from 2.9 to 7 K to find at which temperature and field values the anomaly in R is observed. Fig. 4 shows the R – H curves obtained. For $I = 50$ mA, the dip and rise in R exists only for a narrow temperature region at this current, from 3.5–4.3 K. Above 4.3 K, the anomaly is no longer seen although the curve does have a long tail extending almost to zero field and corresponding to flux flow in the sample. R – H curves were thus obtained at different temperatures and current values to map out the region where the anomaly in the resistance occurs after the onset of superconductivity. Fig. 5 summarises the results obtained from several R – H scans, showing the typi-

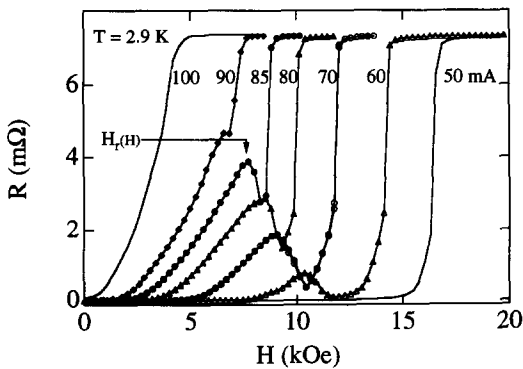


Fig. 3. Resistance vs. applied field at 2.9 K for different measuring currents. The anomaly in the resistance is seen for currents I between 60 and 90 mA appearing at fields between 11 and 6 kOe.

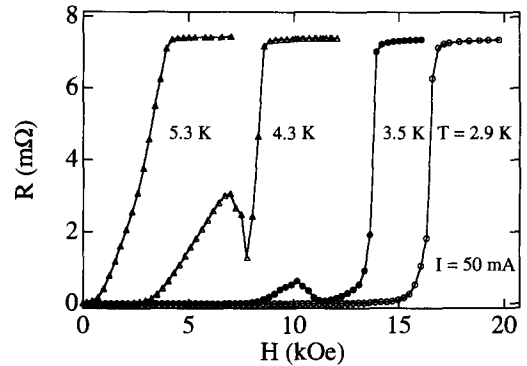


Fig. 4. Resistance as a function of applied magnetic field for different temperatures for a given measuring current of 50 mA. For this particular measuring current, the anomaly in R exists only for a narrow temperature region, $3.5 \text{ K} < T < 4.3 \text{ K}$.

cal current and temperature values at which the anomaly in R vs. H appears. In all cases the curves are reversible (for increasing or decreasing fields). We observed the anomalous rise in resistance from 1.8 K (the lowest temperature at which we could perform our R – H measurements) and the effect persists up to 6.3 K, which is $0.9T_c$. This is very similar to the temperature range over which the peak in the M vs. H curve is seen in these crystals. The resistance anomalies that we observe in $\text{Yb}_3\text{Rh}_4\text{Sn}_{13}$ resemble strongly those reported for NbSe_2 [6] and recently for CeRu_2 [15].

The observation of a peak in the M vs. H curves coupled with a sudden dip and rise in the resistance

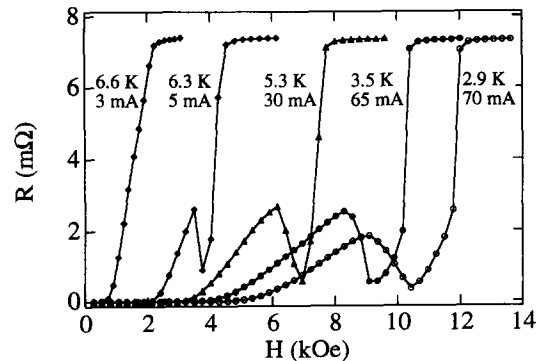


Fig. 5. Resistance vs. magnetic field for different measuring currents at different temperatures showing the extent of the temperature range over which the anomalous increase in R is observed.

after the onset of the superconducting transition, as seen in the $R-H$ curves, would suggest a change in the critical current in the $H-T$ regime defined by these two measurements. In order to investigate this, a measurement of the critical current was undertaken. Voltage as a function of current was measured at different fields and temperatures. The measured voltage shows anomalies for field values corresponding to those seen in the magnetisation and resistance measurements (described above). A typical voltage variation is shown in Fig. 6a at $T = 3.5$ K. The critical current was extracted from these plots using three different criteria; the appearance of 2, 1 or 0.1 μV across the sample. The results are plotted in Fig. 6b for 0.1 μV and the variation is identical to that obtained using the other voltage criteria. The critical current decreases with field as expected, but at high fields, below H_{c2} , it shows a hump before falling to zero at H_{c2} . The hump is very prominent at 5.3 K, while for lower temperatures it appears smeared out (probably due to the larger extent in the field of the enhanced pinning region at lower temperatures). These results differ slightly from the critical current measurements reported on V_3Si , which also exhibits the 'peak effect', where, the hump in the critical current is larger in magnitude and is localised very close to H_{c2} for all temperatures [16].

The $H-T$ phase diagram obtained from all the M vs. H and R vs. H , measurements is presented as Fig. 7. The H_{c2} and H^* values obtained from the magnetisation measurements are shown in the figure which agree well with those obtained by Sato et al. [4]. Assuming that the features seen in the magnetisation are due to changes in the pinning in the sample, it is interesting to see how this relates to the resistance anomalies seen in the $R-H$ measurements. The field at which a resistance anomaly is first seen, at a given temperature and for the minimum measuring current (for example, 60 mA in Fig. 2), can be interpreted as the field required to cause a movement of the flux lines: the Lorentz force exceeds the strength of the pinning force and the flux lines are therefore ripped away from such pinning sites. The resultant flow of flux in the material creates dissipation and hence a voltage appears across the sample. This field, H_r , can be plotted on the same $H-T$ phase diagram to define a field region between a region of easy movement of flux lines (all fields

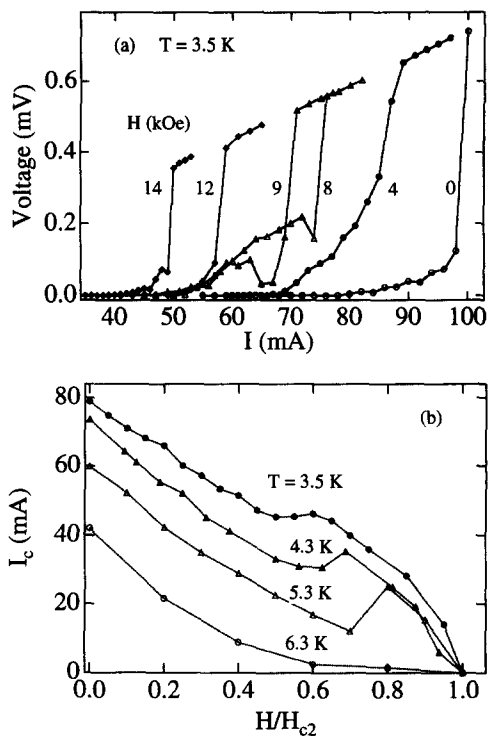


Fig. 6. (a) I vs. V curves at $T = 3.5$ K for different applied fields. (b) Critical current (I_c) variation as a function of reduced magnetic field (H/H_{c2}) at different temperatures. I_c is determined from the criteria that a voltage of 0.1 μV appears across the sample.

below H_r) and a region of strong pinning, where an applied field sets the scale for the lattice parameter of the flux-line lattice but does not move the flux-line lattice from the more energetically favourable pinned configuration (fields above H_r). However, the $H-T$ line obtained from H_r lies below that obtained from the M vs. H measurements, H^*-T . It may be argued that because the observation of the resistance anomaly is dependent on the measuring current, (see Figs. 3–5) the H_r-T line obtained from these measurements is not truly representative of a boundary. In order to see how this H_r-T line relates to the H^*-T line (obtained from M vs. H curves), we have done the following. The values of H_r obtained for several measuring currents at a given temperature (for e.g. 2.9 K) are plotted against the measuring current in the inset to Fig. 7. A simple, linear extrapolation of this curve shows that for zero measuring currents ($I = 0$), the field H_r approaches the

H^* value obtained from magnetisation. A linear extrapolation is not really appropriate, however because of the contrast problem, discussed above, for lower currents it is not really possible to extract sufficient data to accurately model the current dependence of the anomalies in resistance. This analysis of the data however does suggest that these measurements are sampling the same feature observed in the magnetisation measurements. The field values obtained from this simple extrapolation are shown in the figure as H_r^* and lie close to H^* obtained from magnetisation.

The results presented here for $\text{Yb}_3\text{Rh}_4\text{Sn}_{13}$ are very similar to those obtained for CeRu_2 . In both these compounds, viewing just the anomalies in the magnetisation and resistance measurements in isolation, one may conclude that the anomalies are associated with the conventional peak effect seen in many type II superconductors. For CeRu_2 , there exists a body of additional results from magneto-caloric, elastic constant [12] and small angle neutron scattering [17] which provide additional support to the interpretation of the change in the pinning properties in terms of the FFLO state. Results on the $\text{Yb}_3\text{Rh}_4\text{Sn}_{13}$ crystals however are restricted at present to magnetisation and magneto-transport measurements.

To examine the possibility of the H - T line, obtained from the magnetisation and resistance measurements, being a boundary between the conventional superconducting state and the FFLO state, we consider the following. (i) The temperature region over which the FFLO state exists is given as $T \leq 0.55T_c$ by Gruenberg and Guenther [18]. In our experiments on $\text{Yb}_3\text{Rh}_4\text{Sn}_{13}$, the temperature region which shows both the peak effect in magnetisation and the jumps in resistance, extends up to $0.9T_c$. This is also the case in CeRu_2 and UPd_2Al_3 [12]. (ii) The condition that the mean free path (l) is substantially large when compared with the coherence length (ξ) appears to be satisfied in CeRu_2 (at least in some of the samples studied in the literature) as well as in UPd_2Al_3 . For $\text{Yb}_3\text{Rh}_4\text{Sn}_{13}$, our estimate of l , which agrees well with that of Sato et al. [4] is ~ 75 – 80 Å and ξ is ~ 100 Å. This clearly falls outside the 'clean limit' condition for the observation of the FFLO state. (iii) Another condition that $\beta > 1.8$, where β is the strength of the paramagnetic relative to the orbital critical field ($\beta = \sqrt{2}H_{c2}/H_p$) [18], is estimated to be ~ 0.2 for $\text{Yb}_3\text{Rh}_4\text{Sn}_{13}$. CeRu_2 barely satisfies this condition, these values being again sample dependent, whereas β is 2.5 for UPd_2Al_3 . The heavy fermion compounds and CeRu_2 appear to satisfy the conditions (ii) and (iii) but still

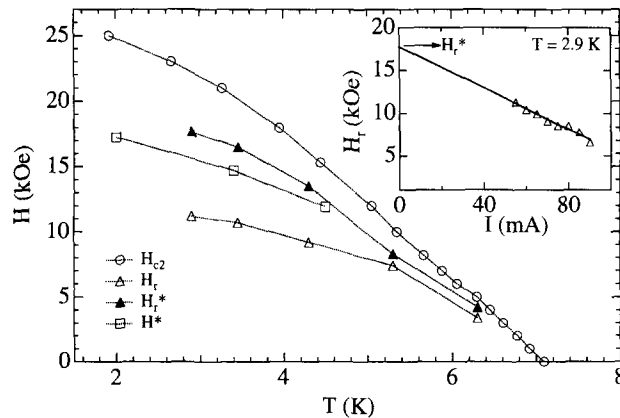


Fig. 7. The H - T diagram for $\text{Yb}_3\text{Rh}_4\text{Sn}_{13}$ obtained from magnetisation and resistance measurements. The H_{c2} values are obtained from resistance measurements. H^* corresponds to the field at which the onset of the peak in magnetisation appears. H_r is the field at which the peak occurs for the minimum measuring current in the R - H measurements (see Fig. 3). The inset shows the plot of H_r for various measuring currents at a given temperature. It can be seen that the extrapolated value of H_r for $I = 0$, approaches H^* , and is plotted as H_r^* in the figure.

fall short of condition (i) for the observation of the FFLO state. Even in these compounds it is still not entirely clear whether the FFLO state exists or not, despite extensive experimental investigations. A more detailed discussion of the interpretation of the experimental observations in the heavy fermion and related compounds can be found in a few recent publications [19–22].

However, attempts at producing a more realistic model of the FFLO state by Tachiki et al. [23,24] have led to the postulation of the generalized FFLO model, GFFLO [23,24]. Within the framework of the GFFLO model, the region of H – T phase diagram where a FFLO state exists, may extend to temperatures higher than the $T \sim 0.55T_c$ predicted by the original FFLO theory [8,9,18] and a degree of pinning is required for the observation of the new state. Therefore, in perfect samples it may not be possible to observe the FFLO state through resistivity measurements, for instance. Slightly imperfect specimens may however pin the fragmented flux lines and thus allow an experimental observation of the formation of the FFLO state. The new generalized FFLO state proposed by Tachiki et al. [23,24] is now being invoked to understand the pinning properties exhibited by compounds such as CeRu₂, UPd₂Al₃ and V₃Si [19–22].

Information about the morphology and quality of the flux-line lattice (FLL) of these superconductors in the mixed state can be obtained from neutron small angle scattering investigations. Since this may be the only way to gain a microscopic picture of the changes in the flux distribution in materials which might exhibit a FFLO state, we reiterate the conclusions of these experiments on CeRu₂ [17]. Diffraction studies of the FLL in high quality samples of CeRu₂ may be interpreted in terms of a strongly fractured lattice of flux lines with the longitudinal correlation length greatly exceeding the transverse equivalent. The applied field dependence of the transverse correlation length can be described reasonably by a weak collective pinning model with a pin spacing of similar magnitude to that which the FLL achieves near to H_{c2} . The integrated intensity of the Bragg reflections from the FLL show a marked reduction above H^* but a lattice is still observed at higher fields. This effect may be due to core interactions modifying the field distribution within the sam-

ple and hence reducing the contrast for the neutron diffraction. Studies of the FLL in Yb₃Rh₄Sn₁₃ crystals are planned and will help to illustrate the nature of the transitions observed in these experiments.

In Yb₃Rh₄Sn₁₃, we observe a transition from a weakly pinned regime at low fields to a strongly pinned regime at high fields. This strongly pinned region does not extend all the way to T_c , but vanishes at temperatures around $0.9T_c$. This cut-off temperature is the same, both from the M – H and R – H measurements. Regions of strong pinning can arise due to various factors, one of them being the presence of disorder in the crystal giving rise to pinning centres of dimension greater than ξ . In the Yb₃Rh₄Sn₁₃ crystals, disorder cannot be entirely ruled out due to the various modifications of the phase I crystal structure that can occur (see Section 1). A 'matching' of the FLL spacing to the separation of such pinning centres would then occur at a particular field giving rise to an abrupt increase in pinning. In our study, we observe this abrupt increase in the pinning to have a temperature dependence as well, the H_r – T line which is flat at low temperatures, falls to lower fields at higher temperatures (see Fig. 7).

In summary, from our results of magnetisation, resistance and critical current measurements, we confirm that there is a region in the H – T phase diagram that shows increased pinning at high fields. A region of strong irreversibility is observed in the $M(H)$ curves at high fields just below H_{c2} . The application of a field does not merely cause a broadening of the resistance transition, but for high fields, an abrupt dip and rise in the resistance is observed before approaching $R = 0$. This region is associated with an abrupt reduction in the dissipation caused by the flux-flow motion. When further examined by critical current measurements as a function of field, a hump is observed at fields lower than H_{c2} . Although Yb₃Rh₄Sn₁₃ appears to fall short of the criteria put forward for the observation of the FFLO state, the features seen in magnetisation and resistance measurements cannot entirely be explained as being due to the conventional peak effect. It is not clear as yet whether the enhanced pinning region exhibited by this compound can be understood within the new generalised FFLO state proposed by Tachiki et al. [23,24]. This model would at least appear to explain

the extended temperature region over which the peak effect is observed in $\text{Yb}_3\text{Rh}_4\text{Sn}_{13}$.

Acknowledgements

We would like to thank the IRC in Superconductivity, University of Cambridge, for the use of the SQUID and VSM, and Doug Astill for his help during these measurements. This work was supported by a grant from the EPSRC, UK.

References

- [1] J.P. Remeika, G.P. Espinosa, A.S. Cooper, H. Barz, J.M. Rowell, D.B. McWhan, J.M. Vanderberg, D.E. Moncton, Z. Fisk, L.D. Woolf, H.C. Hamaker, M.B. Maple, G. Shirane, W. Thomlinson, *Solid State Commun.* 34 (1980) 923.
- [2] J.L. Hodeau, J. Chenavas, M. Marezio, J.P. Remeika, *Solid State Commun.* 36 (1980) 839.
- [3] J.P.A. Westerveld, D.M.R. Lo Cascio, H. Bakker, *J. Phys. F* 17 (1987) 1963.
- [4] H. Sato, Y. Aoki, H. Sugawara, T. Fukuhara, *J. Phys. Soc. Jpn.* 64 (1995) 3175.
- [5] A.M. Campbell, J.E. Evetts, *Adv. Phys.* 21 (1972) 327; A.B. Pippard, *Phil. Mag.* 19 (1969) 217.
- [6] S. Bhattacharya, M.J. Higgins, *Phys. Rev. B* 49 (1994) 10005; K. Ghosh, S. Ramakrishnan, A.K. Grover, G.I. Menon, G. Chandra, T.V.C. Rao, G. Ravikumar, P.K. Mishra, V.C. Sahni, C.V. Tomy, G. Balakrishnan, D.McK. Paul, S. Battacharya, *Phys. Rev. Lett.* 76 (1996) 4600.
- [7] U. Yaron, P.L. Gammel, D.A. Huse, R.N. Kleiman, C.S. Oglesby, E. Bucher, B. Batlogg, D.J. Bishop, K. Mortensen, K. Klausen, C.A. Bolle, F. de la Cruz, *Phys. Rev. Lett.* 73 (1994) 2748; G. D'Anna, M.V. Indenbom, M.-O. Andre, W. Benoit, E. Walker, *Europhys. Lett.* 25 (1994) 225.
- [8] P. Fulde, R.A. Ferrel, *Phys. Rev.* 135 (1964) A550.
- [9] A.I. Larkin, Y.N. Ovchinnikov, *Sov. Phys.-JETP.* 20 (1965) 762.
- [10] K. Gloos, R. Modler, H. Schimanski, C.D. Bredl, C. Geibel, F. Steglich, A.I. Buzdin, N. Sato, T. Komatsubara, *Phys. Rev. Lett.* 70 (1993) 501.
- [11] A.D. Huxley, C. Paulsen, O. Laborde, J.L. Tholence, D. Sanchez, A. Junod, R. Calemczuk, *J. Phys-Condens. Matter* 5 (1993) 7709.
- [12] Y. Onuki, M. Hedo, Y. Inada, R. Settai, H. Suguwara, Y. Aoki, H. Sato, M. Deppe, P. Gegenwart, C. Geibel, M. Lang, T. Luhmann, R. Modler, M. Weiden, F. Steglich, C. Paulsen, J.L. Tholence, N. Sato, T. Komatsubara, M. Tachiki, S. Takahashi, *Physica B* 223–224 (1996) 28 and references therein.
- [13] G.P. Espinosa, *Mater. Res. Bull.* 15 (1980) 791.
- [14] M. Isino, T. Kobayashi, N. Toyota, T. Fukase, Y. Muto, *Phys. Rev. B* 38 (1988) 4457.
- [15] N.R. Dilley, J. Herrmann, S.H. Han, M.B. Maple, S. Spagna, J. Diederichs, R.E. Sager, *Physica C* 265 (1996) 150.
- [16] N.E. Alekseevskii, N.M. Dobrovolskii, A.V. Dubrovnik, E.P. Krasnoperov, V.A. Marchenko, *Sov. Phys. Solid State* 17 (1976) 1349.
- [17] A. Huxley, R. Cubbit, D.McK. Paul, E. Forgan, M. Nutley, H. Mook, M. Yethiraj, P. Lejay, D. Caplan, J.M. Penseisson, *Physica B* 223–224 (1996) 28.
- [18] L.W. Gruenberg, L. Guenther, *Phys. Rev. Lett.* 16 (1996) 996.
- [19] P. Gegenwart, M. Deppe, M. Koppen, F. Kromer, M. Lang, R. Modler, M. Weiden, C. Geibel, F. Steglich, T. Fukase, N. Toyota, *Ann. Phys. Leipzig* 5 (1996) 307.
- [20] F. Steglich, R. Modler, P. Gegenwart, M. Deppe, M. Weiden, M. Lang, C. Geibel, T. Luhmann, C. Paulsen, J.L. Tholence, Y. Onuki, M. Tachiki, S. Takahashi, *Physica C* 263 (1996) 498.
- [21] R. Modler, P. Gegenwart, M. Lang, M. Deppe, M. Weiden, T. Luhmann, C. Geibel, F. Steglich, C. Paulsen, J.L. Tholence, N. Sato, T. Komatsubara, Y. Onuki, M. Tachiki, S. Takahashi, *Phys. Rev. Lett.* 76 (1996) 1292.
- [22] R. Modler, *Czech. J. Phys.* 46 (1996) 3123.
- [23] M. Tachiki, S. Takahashi, P. Gegenwart, M. Weiden, M. Lang, C. Geibel, F. Steglich, R. Modler, C. Paulsen, Y. Onuki, *Z. Phys. B* 100 (1996) 369.
- [24] M. Tachiki, T. Koyama, S. Takahashi, *Physica C* 263 (1996) 1.